High-Efficient Bladeless Expander Concept

Avinash Renuke[1*], *Federico* Reggio[2], *Alberto* Traverso[2], *Matteo* Pascenti[2], and *Paolo* Silvestri[3]

[1]Malardalen University, Vasteras, Sweden
[2]University of Genoa, Genoa, Italy
[3]SIT Technologies srl. Genoa, Italy

Abstract. Tesla bladeless expanders are promising in energy harvesting and small-scale power generation applications due to their lower cost and simplicity in design. Although such expanders exhibit very high rotor efficiency (analytical total to static efficiency ~ 90%), it shows poor performance when coupled with a stator (experimental total to static efficiency ~30%) due to losses present in the stator and stator-rotor interaction. This paper presents the design and experiment of a novel, high-efficient Tesla bladeless expander concept. The concept arises from the loss phenomena in the stator-rotor interaction in conventional bladeless expanders, which are among the main causes of the low performance. This concept is believed to bring the bladeless expanders to the same performances as the traditional ones with vanes, compared to which however the bladeless machines boast greater simplicity, robustness, and the absence of performance decay as the size decreases, competing even in the contexts for traditional turbomachinery. The high-efficient bladeless expander prototype with water as a working fluid is designed and developed, representing the similitude case for a liquid butane heat pump. The available isentropic power across the throttling process in the butane case is 3.3 kW @10000 rpm. The turbine consists of 24 nozzles and 150 disks separated by 0.1 mm spacers. The turbine shaft is connected to the high-speed electric generator. The performance test on the expander is carried out at rotational speeds ranging from 3000 rpm to 6200 rpm and with differential pressure across the expander up to 14 bar. Experimental ventilation loss is characterised and its effect on the performance of the expander is discussed. The preliminary results of the expander under investigation showed satisfactory production of power with an acceptable efficiency range. It is also shown that the present concept is promising and able to address the major i.e., stator-rotor interaction which is the major source of loss in the traditional bladeless expander.

1 Introduction

1.1 Background and Motivation

Tesla [1][2] created the bladeless turbomachines, commonly referred to as Tesla turbomachines, in the early 19th century. It consists of thin disks with a central hole that are spaced apart and positioned parallel to the shaft. Fluid enters the rotor tangentially in turbine mode and exits the rotor axially at the central hole. In compressor mode, fluid enters through the disk's central holes and exits through their edges. The external volute is then used to convert the peripheral high-speed fluid into static pressure. As a result, this machine is reversible; by switching the rotor's direction of rotation, the turbine and compressor modes can both be controlled by the same machine. Comparatively speaking to traditional bladed turbines, the relative velocity between the fluid and the disk is quite low. The flow inside the rotor is laminar because of its lower relative velocity. The Tesla turbine's internal laminar flow field is essential for an efficient energy transfer between the fluid and the disk. Through shear force, the fluid layers that are sandwiched between the disk gaps transfer energy. This shear produces a drag force on the disk that is directed in the direction of rotation. As a result, viscous shear drag on the Tesla rotor works in the generating power as opposed to the bladed turbine, where it works against the rotor's propulsion. Numerous academics have been drawn to explore bladeless turbines as a result of this intriguing occurrence.
Tesla asserted that his rotors could operate at up to 97% efficiency. Researchers have also provided analytical support for this [3][4], however, according to experimental results, the total Tesla turbine efficiency (stator + rotor) is only about 35-40% [5]. One of the main causes for the Tesla turbine's lack of commercial success up to this point is its poorer efficiency when compared to traditional bladed turbomachinery.

* Corresponding author: avinash.renuke[at]mdu.se

The advantages of the Tesla turbine like resistance to erosion [9], low noise [10], reversibility of the flow[1][2], simple and economic in construction and flexibility in the choice of fluid make it well suited for energy harvesting and small-scale power generation application. In recent times, a renovated interest in Tesla machinery is clearly emerging. It has to be remarked how the trend is drastically increasing in the last few years; this is directly linked to the high attention that micropower generation gained in the energy market, where Tesla turbines have attractive features, mainly for their high cost-effectiveness and relatively simple manufacturing. However, there are no established criteria yet for Tesla machinery design, and many Authors and practitioners work on very small prototypes (~100-1000W scale), where manufacturing tolerances and uncertainties in losses may hinder the accuracy of experimentation.
There is a need for a structured effort towards the Efficient and well-designed, at least, kW size Tesla machinery, for untapping their potential in becoming one of the players in turbomachinery technologies, where their features are competitive or more promising than other conventional machinery.

1.2 High-efficient bladeless turbomachine concept

In this article, we present the concept for improvement of the performance of the bladeless expander and analyse it through experiments. We propose a high-efficient bladeless turbomachinery design which is based on the detailed understanding of the losses studies in our previous experimental works [6]. Through such detailed experimental characterization, it was possible to identify, for the first time, the major sources of losses, which are: i) stator-rotor interaction and ii) leakages. While the latter can be solved with conventional sealing elements, under customization now for the prototype, the former represents an inherent loss present already in the original Tesla patent of 1913 and affecting all the consequent designs and realizations worldwide until now.
The water expander studied in this section is designed based on the high-performing novel "high-efficient" bladeless concept developed based on the deep understanding of the stator-rotor loss phenomenon investigated on bladeless turbomachinery on the previous air prototypes [5][6]. The core innovation of this prototype focused on reducing the loss mechanism contributing most to the performance. In fact, one of the reasons why bladeless turbomachinery hasn't been successful commercially is the experimental low efficiency. This is due to the requirement of highly tangential flow at the inlet of the rotor. The present concept reduces the losses between stator-rotor significantly by ensuring a lesser wetted surface available for the tangential flow between stator-rotor regions. This innovation improves the performance of the bladeless turbine/compressor to the level of conventional bladed machinery, making it now compete with conventional machinery not only at a lower scale (where bladed machinery suffers high losses, differently from bladeless machinery) but also at a large scale.
Unlike many inventors who have tried to improve the performance of the Tesla turbomachines by introducing complex features on the disks themselves, increasing the complexity of the original bladeless Tesla design, the present concept only adds external simple features to the original Tesla's bladeless turbomachinery. These features are simple to manufacture and straightforward to implement without introducing additional complexity to the original bladeless design.

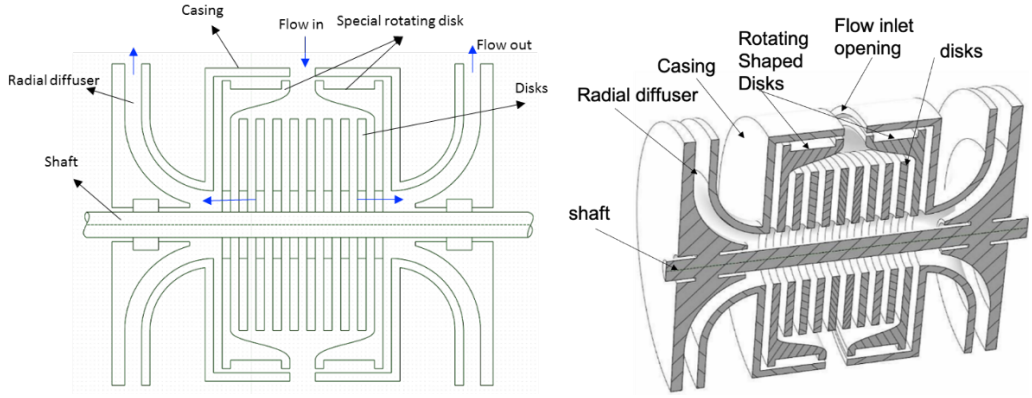

Fig. 1. Schematic diagram of Ultra Efficient Bladeless Expander

The key principle of this concept is to guide the fluid flow with uniform tangential velocity to the rotor. This is obtained with the help of two rotating-shaped disks, as shown in Fig. 1, mounted on both sides of the rotor. Regarding radial stator, flow is accelerated through a radial stator and directed towards the rotor gaps, where flow passes and exchanges momentum, from the disk tip entry to the disk inner discharge. Differently from conventional Tesla machinery, where the radial stator passages, located at the periphery of the rotating disks, have an axial dimension close to the rotor disk ensemble, here the stator has a reduced axial dimension, for instance, half, and the statoric jets are not directed immediately towards the rotating disks, but they first enter a rotating "swirl chamber". Such a chamber is created by two special rotating shaped disk/s, symmetrically mounted on the

shaft, shaped in such a way that they form a rotating radial passage to drive the fluid from the stator to the rotating disks. In this way, a significant radial distance exists, for instance, 10% of the disk tip radius, between the stator and the rotating disk ensemble: as a consequence, friction between the rotating disk ensemble and stator or casing is minimised, reducing friction losses between rotor and stator.
The prototype, which experimental results are described hereby, has been designed to perform a demonstration of a liquid Tesla expander for heat pump application conditions. The design point case used to demonstrate the present "high-efficient" Tesla turbine is for the expansion of butane as a working fluid. As the expansion is in the liquid phase (incompressible fluid), therefore we consider water (safe – incompressible fluid) for performance demonstration applying similitude considerations to later transfer the results to the liquid butane expansion case. Therefore, considering the derived butane thermodynamic conditions, targeting a water prototype design as close as possible to such butane thermodynamic conditions, the following design point is formulated.

Table 1. Thermodynamic design specification.

Thermodynamic data	Demonstration design data
Working fluid	water
dp across turbine, bar	14
Rotational speed, rpm	10000
Mass flow, kg/s	2
Power, W	1400 (expected)
Efficiency, %	70+ (expected without leakage, ventilation and bearing loss)

2 Experimental analysis

2.1 Turbine components and test rig

In this section, experimental tests of a water expander with "High-Efficient" Tesla rotor design is presented. The turbine specifications are reported in Table 2.

Table 2. Thermodynamic design specification.

Stator	3D printed nozzles – 5 deg angle
Number of nozzles	24
Rotor disk outer diameter, mm	80
Rotor disk inner diameter, mm	32
Disk discharge section holes	3
Disk thickness, mm	0.1
Disk gap, mm	0.1
Number of disks	150

The different components of the water expander can be seen in Fig. 2 and 3. The turbine consists of the following main components:
1. Inlet port: inlet port is the inlet piping connection for the water to enter the turbine. Water from the inlet port enters into nozzles. There are two inlet ports used in this turbine.
2. Stator: there are 24 nozzles placed around the circumference of the rotor, which increase the velocity of the incoming water. High-speed jets of water enter the rotor. Stator is manufactured using 3D printing technology into one single piece.
3. Rotor: turbine rotor consists of thin metal disks parallelly mounted on the shaft. The disks are separated by spacers, which maintain the desired gap between disks along with rotating shaped disks.
4. Radial diffuser: radial diffuser at the exit of the turbine is used to convert the exit kinetic energy of the water into pressure energy.
5. Collector: the water coming out of the radial diffuser has tangential velocity and to redirect the flow into a single channel/pipe, a collector is used. The role of the collector is to smoothly transfer water from the radial diffuser to the exit pipe.

This Tesla turbine was designed to operate at speeds up to 10,000 rpm. Given the need to seal the turbine casing, the rotor has a cantilevered (as shown in Fig. 3(b)) arrangement to allow the use of a single mechanical seal. The mechanical seal has been placed to avoid the water exit where the 15mm diameter shaft is coming out of the turbine casing for connecting to the generator through a joint. The rotor is supported by three spindle bearings placed on the generator side between the mechanical seal and the joint, while on the opposite side, the cantilevered disc pack is held together by a shaped ring nut. The turbine has 3 chambers: the cylindrical inlet manifold, connected externally to the 2 inlet pipes, surrounds the stator and the chamber containing the rotating discs, finally

the liquid that comes out of the turbine is collected in an exhaust manifold and exits from the 2 pipes drain. All the machine components are kept together by flanges and 6 threaded rods with a 12mm diameter.
Fig. 3(c)(d) shows the rotor and stator assembly. Stator is made with plastic as well as metal using 3D printing technology. Figure 4 shows the whole assembly of the expander with inlet and exhaust piping arrangements. The following measurements are done to evaluate the performance of the turbine – inlet pressure, outlet pressure, mass flow using the ultrasonic instrument for greater accuracy and generator power using current and torque convertor factors provided by the manufacturer.

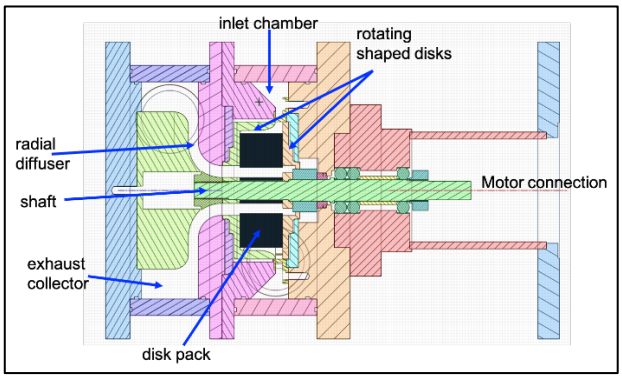

Fig. 2. 3D drawing of water 1kW expander

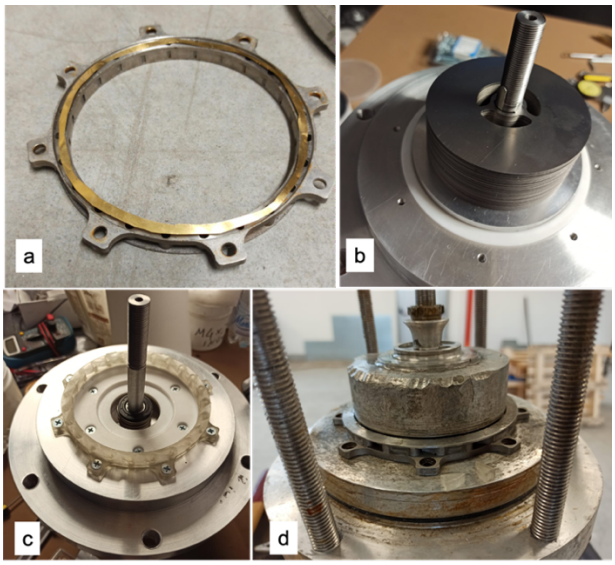

Fig. 3. Water Tesla expander components: (a) metallic stator, (b) rotor assembly, (c) rotor with plastic stator, (d) rotor with metallic stator

Fig. 4. Water expander experimental test rig

The experimental test rig is shown in Fig. 4. The inlet pressure to the turbine is provided by a high-pressure water pump to achieve the pressure difference between the turbine inlet and turbine exit as shown in Fig. 4. The tests

are performed by varying the capacity of the pump (0% pump means that we are feeding with the laboratory line pressure). The turbine exit is subject to higher than atmospheric pressure due to discharge line pressure drops.

2.2 Measurement and performance parameters

The performance of the turbine is measured using the following sensors:
Pressure sensors: Two static pressure probes are used: one at the inlet pipe and one at the exit pipe after the collector.
Mass flow sensor: Ultrasonic mass flow sensor is used for better accuracy to measure the mass flow at the exit line of the turbine.
Inverter: Generator output signals have the rotational speed and current (converted to torque is the torque conversion coefficient given by the manufacturer).
All sensors and inverter signals are connected to a laboratory data acquisition system through which all data is monitored and recorded. Turbine performance is evaluated mainly in terms of total to static efficiency and power. Power is calculated using torque applied by the electrical rotor (therefore electrical losses are not considered) and angular velocity as:

$$P = \tau * \omega \tag{1}$$

Where, P is power (Watts) , τ is torque (N.m) and ω is amgular velocity (rad/s). Torque in N-m is evaluated by measuring the RMS current output (I) of the generator and using the conversion factor given by the generator manufacturer.

$$\tau = I * 0.344 \tag{2}$$

The efficiency of the turbine is calculated using the following equation,

$$\eta_{exp} = \frac{P_{exp}}{Q * \Delta p} \tag{3}$$

Where, η_{exp} Total to static efficiency, calculated based on diffuser exit, Q is volume flow rate in m3/s and Δp is the pressure difference across turbine in Pascals.

2.3 Uncertainty analysis

Equations (2) and (3), which are evaluated using measurable quantities including static pressure, rotating speed, mass flow, and current, are used to compute the expander's efficiency and power. The function that links the result to these parameters causes uncertainties resulting from instrumental error, calibration error, and random error to affect each of these numbers. Instrumental errors digitally recorded values can be considered negligible. The experiment is repeated under identical circumstances, with the same user, and with various rotational speeds and input pressures to accommodate the random error. In this scenario, curves are obtained three times. The method of root sum squares is used to determine the combined error. The uncertainty of a given function h with n direct measures, $h = f(x_1, x_2, x_3, ..., x_n)$, can be calculated as follows:

$$\sigma_g = \sqrt{\sum_{i=1}^{n} \cdot \left(\frac{dh_i}{dx_i}\Delta x_i\right)^2} \tag{4}$$

where σ_g is the uncertainty observed in the output of function h, while Δxi is the uncertainty in i^{th} measure.
Table 3 shows the uncertainty in the instruments used in the experimental analysis. To account for the 95.5% confidence interval, the standard deviation for all repeated measurements is taken into consideration as ±2 SD. The calculated uncertainty for power is ±3.5 W. The maximum uncertainty in efficiency is ±1.25% and the uncertainty at the maximum efficiency point is ±0.89%.

Table 3. Measurement accuracies of sensors

Sensors	Range	Accuracy
Turbine inlet pressure	0 - 25 bar	±0.5 %
Turbine exit pressure	0 - 6 bar	±0.25%
Mass flow	0 - 5 kg/s	±1.5%
Generator current	0 - 9 A	±0.5%

Rotational speed	0-15krpm	±0.1%

2.4 Results and Discussion

Experiments are performed by varying pump capacity. 0% pump capacity refers to the flow due to the supply line pressure in the lab which has positive pressure. At a fixed pump capacity (i.e., almost fixed turbine inlet water pressure), the power of the turbine is obtained at different rotational speeds. The turbine seed is kept below 10000 rpm to avoid critical speed regions. The rotor dynamics analysis on this rotor is performed according to methods used for previous bladeless rotors [7].

Figure 5 shows efficiency and power versus rotational speed at different pump capacities, which mainly impacts on the turbine inlet pressure. As the pressure at the turbine exit (collector exit) is measured, total to static efficiencies based on diffuser exit (η_{exp}), are calculated. Figure 5 shows that maximum turbine efficiency (η_{exp}), 29.5%, is obtained at 2.87 kg/s mass flow at 3000 rpm i.e., higher than the design mass flow (2 kg/s). The design mass flow of 2 kg/s is assumed (according to numerical calculations) to enter completely inside the rotor and does not bypass the rotor as a leakage flow. In the experimental analysis, some flow bypasses the rotor through the end disk gap without producing any power. It may be possible that there is high leakage across the rotor of the turbine due to which maximum efficiency is obtained at a higher total mass flow. Another major possibility for the lower performance of the turbine is ventilation loss, which is evaluated in the next section.

For all the operating curves, peak efficiency is obtained at lower rotational speeds and higher mass flow. This turbine performance can be explained in the following way: at low rotational speeds, mass flow through the turbine is higher which ensures the velocity ratio is greater than 1. Therefore, we see positive power at lower rotational speeds as seen in Fig. 5. Hence the peak efficiencies are obtained at lower rotational speeds. At the same time, the lower speed causes a lower-then-design pressure at the rotor tip, which causes a higher pressure drop across the throat, and hence a higher overall mass flow.

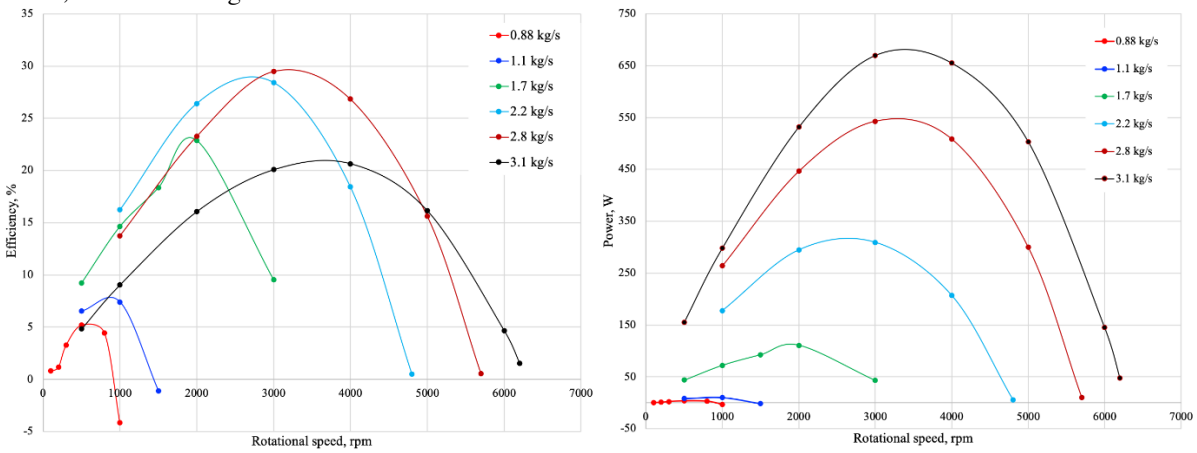

(a) (b)

Fig. 5. (a) Total to static efficiency versus rotational speed; (b) mechanical power versus rotational speed at different mass flow for water expander

3 Loss analysis

As seen in section 2.4, the performance of the expander was not as expected by numerical results. In order to understand the cause, as the first intuition for the major source of losses, ventilation loss (viscous shear friction between end rotating disks and casing as shown in Fig. 6, due to the higher available surface of rotating parts with respect to casing, the run-down experiment is performed. The run-down experiment is performed both with air (i.e. empty turbine) and with water.

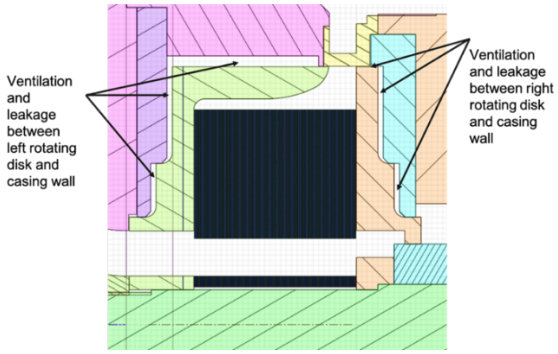

Fig. 6. Ventilation loss passages in turbine

Figure 7 shows the run-down test performed with both air and water. The run-down test is performed in a similar way as done for previous air expanders [5][6][8], in which the turbine is rotated at the desired speed and then the mass flow is cut down so that the turbine decelerates due to viscous friction loses and mechanical losses present in the turbine. Rotational speed and time is recorded during the deceleration of the turbine. A run-down test with air on the current expander gives a clear understanding of losses due to mechanical sealing and the bearings. This is because, as the gap between the rotating surface and casing is ~1 mm, we expect ventilation power loss would be negligible in this case. Run down is started with the rotational speed of 5500 rpm and when the water supply is cut off, the rotor comes to rest due to viscous resistances in the stator-rotor cavity. In the case of air, the rotor is brought to 5500 rpm using a generator because there are no inlet air flow arrangements in the water test rig.

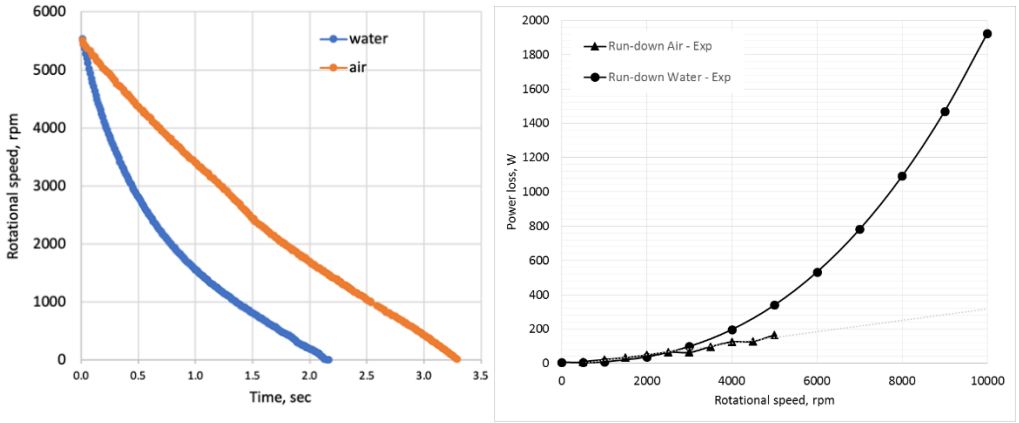

(a) (b)

Fig. 7. (a) Run down test with water and air; (b) Power loss with respect to speed

Figure 7 also shows the run-down test data calculated in terms of ventilation power with respect to rotational speed. The ventilation loss for water shows a strong quadratic trend with respect to rotational speed. We can see that ventilation losses are significant if we compare the design power of the machine, which is 1.4 kW @10000 rpm. The ventilation power loss is greater than the design power. Hence there is no production of positive power at a higher rotational speed. The positive power produced by the turbine at lower rotational speed, as shown in Fig. 7, is due to lower ventilation losses. On the other hand, when the turbine is empty and it's rotating in the air, it is clear that ventilation viscous losses are now much lower. The ventilation power loss in the air represents the mechanical power loss in the expander. This is validated as the mechanical seal used in the expander has a nominal power loss of 300 W @10000 rpm as per the seal catalogue. Hence, when water is present, the major source of losses in the expander is ventilation loss due to rotating surfaces and casing.

Experimental tests have allowed demonstrating shaft powers (Figure 7) close to the design ones (1kW), reduced however by the presence of ventilation losses at the ends of the rotor, due to viscous friction with the walls of the turbine casing: these losses have been quantified experimentally and can be significantly reduced by means of typical turbomachinery solutions. Assuming that ventilation losses can be made negligible, it was possible to estimate the efficiency curves relating to the power actually extracted from the fluid, as shown in Figure 8: since no Tesla turbine prototype has ever exceeded 40% isentropic shaft efficiency rotating, in the international technical literature, one can guess the interest that the present invention can arouse, being able to reach and exceed values of more than 60%.

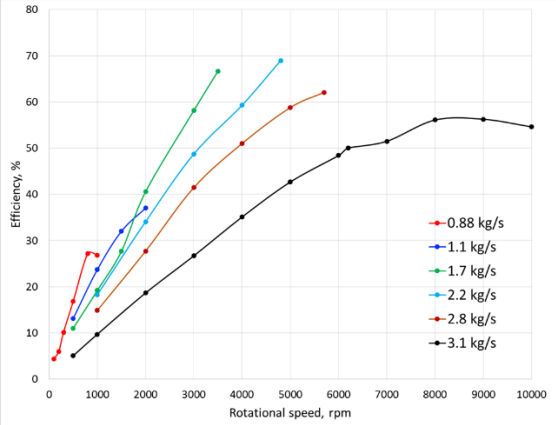

Fig. 8. Efficiency obtainable by eliminating ventilation losses, as a function of rotation speed and for different flow rates

Figure 8 shows the experimental performance without ventilation losses. It can be observed that the curves at mass flow 1.7 kg/s and 2.2 kg/s are approaching efficiency higher than 70%. This suggests that if the ventilation losses are reduced, the expander performance matches with numerical performance. In the near future, the validated 2D/3D numerical model can be used to optimise and reduce the power loss due to ventilation, applying conventional approaches (e.g., increase in clearance and high surface finish) as well as innovative concepts (e.g., superficial features).

4 Conclusion

A novel concept to improve the performance of Tesla expander is presented in this article. The experiment is performed at design point pressure and off-design conditions for different rotational speeds and pressure drops across the expander. The maximum efficiency of 29.5% is recorded and the maximum power of 660 W at 3200 rpm. The maximum rotational speed reached by the turbine was 6500 rpm. This is mainly due to ventilation losses between end rotating disks and casing. Experimental ventilation loss characterisation is performed to estimate the power lost due to ventilation. Results showed very high ventilation loss, >1 kW @8000 rpm (design speed). Due to very high ventilation losses, the turbine could not reach the design speed. However, the results show that the present concept eliminated the traditional stator losses present in the Tesla machines. The ventilation losses could be later reduced by traditional approaches.

This project has received partial funding from the European Union's Horizon 2020 research and innovation programme under grant agreement No 963576.

References

1. Tesla, N., *Turbine*, US Patent 1061206 (1913)
2. Tesla, N., *Fluid Propulsion*, US Patent 1061142 (1913)
3. Armstrong, J. H., *An Investigation of the Performance of a Modified Tesla Turbine*, Ph.D. Thesis, Faculty of the Division of Graduate Studies, Georgia Institute of Technology, USA (1952)
4. Beans, E. W., *Performance Characteristics of a Friction Disk Turbine*, *Ph.D Thesis*, The Pennsylvania State University, USA (1961)
5. Renuke, A., Vannoni, A., Traverso, A., and Pascenti, M., *Experimental and Numerical Investigation of Small-Scale Tesla Turbines*, *ASME. Journal of Engineering Gas Turbines Power*, Vol. 141(12), 121011 (2019)
6. Renuke, A., Reggio, F., Ferrando, M., Pascenti, M., and Traverso, A., *Experimental Characterization of Losses in Bladeless Turbine Prototype*,. *ASME. Journal of Engineering Gas Turbines Power,* GTP-21-1519 (2021)

7. Silvestri, P., Traverso, A., Reggio, F., and Efstathiadis, T, *Theoretical and Experimental Investigation on Rotor Dynamic Behavior of Bladeless Turbine for Innovative Cycles*, Proc of ASME TurboExpo 2019, Vol 3, Phoenix, Arizona, USA. June 17-21. V003T06A025 (2019)
8. Renuke, A., Reggio, F., Pascenti, M., Silvestri, P and Traverso, A., *Experimental Investigation on a 3 kW Tesla Expander With High Speed Generator*, *ASME. TurboExpo'20,* GT2020-14572, London, England (2020)
9. Patel, N., Schmidt, D.D., 2002, Biomass Boundary Layer Turbine Power System", Proceedings of International Joint Power Generation Conference, Phoenix, USA.
10. Tiwari R.N., Niccolini Marmont Du Haut Champ C.A., Reggio F., Silvestri P., Traverso A., Ferrari M.L., "Acoustic signature analysis of a bladeless blower" Applied Acoustics, 208, art. no. 109382, DOI: 10.1016/j.apacoust.2023.109382 (2023)